EVOLUTION & DEVELOPMENT 7:6, 528–541 (2005)

Development of the caudal exoskeleton of the pliomerid trilobite *Hintzeia plicamarginis* new species

Andrew G. Simpson,[a] Nigel C. Hughes,*[,a] David C. Kopaska-Merkel,[b] and Rolf Ludvigsen[c]

[a]Department of Earth Sciences, University of California, Riverside, CA 92521, USA
[b]Geological Survey of Alabama, P.O. Box 869999, Tuscaloosa AL 35486-6999, USA
[c]Denman Institute for Research on Trilobites, Box 322, Moberly Lake, BC, Canada V0C 1X0
*Author for correspondence (email: nigel.hughes@ucr.edu)

SUMMARY The later juvenile ontogeny of the caudal plate of the early Ordovician pliomerid trilobite *Hintzeia plicamarginis* new species likely comprised an initial phase during which the rate of appearance of new segments subterminally exceeded that of segment release into the thorax, a short phase of constant segment numbers, and a later phase during which release occurred but in which no new segments appeared. A distinct terminal region became manifest in the second phase. During the second and third phases growth coefficients for individual segments were about 1.1–1.2 per instar. Although the shapes of segments varied during growth, the pattern of ontogenetic shape change appears to have been broadly similar among segments. This suggests an homonomous trunk segment morphology regardless of thoracic or caudal identity in maturity. These results imply that control of trunk exoskeletal segment appearance and articulation were decoupled in this trilobite, and that the terminal region had a distinct mature morphology. *H. plicamarginis* is described as a new species.

INTRODUCTION

Connecting patterns of growth seen in fossils at the organ or organismal scales to developmental mechanisms operating at the molecular and cellular levels presents a severe challenge. Inferences are strongest when the developmental basis of morphological patterns seen in fossils are conserved across members of crown groups that include the fossils of interest. For example, the sequential appearance of additional exoskeletal segments near the terminus of the trilobite trunk region is accepted to be homologous with the postembryonic appearance of skeletal segments in extant anamorphic arthropods (Størmer 1942; Hessler 1962; Hu 1971), and it is likely that some aspects of the regulation of trilobite trunk segments were shared with those common to living arthropods.

During the meraspid phase of growth (Fig. 1), trilobites constructed the thoracic portion of the trunk via the progressive release of segments from a caudal plate (known during this growth phase as the "transitory pygidium") composed of conjoined segments (as first documented in *Shumardia* by Stubblefield 1926, see also Fortey and Owens 1991). This pattern of growth was apparently unique to the trilobites and their close relatives and was perhaps synapomorphic for an extinct "trilobitomorph" clade of arthropods that bore an exoskeletal caudal plate in maturity (Cotton and Braddy 2004). Trilobite ontogeny demonstrates that the onset of segment articulation could develop long after the initial expression of trunk segments: also a condition not seen in living arthropods. This exchange of segments between caudal and medial regions is remarkable because the caudal plate has commonly been considered to represent a separate tagma and is equated to the abdomen of other arthropods (e.g., Cisne et al. 1980). Exchange of segments between an "abdomen" and a "thorax" represents a highly unusual growth pattern among arthropods (but see Waloszek and Maas 2005) and is thus of interest with regard to the evolution of arthropod body patterning. Therefore, a detailed understanding of the development of the trilobite caudal plate is important not only for understanding an extinct clade, but may also provide insights into the evolution of arthropod body patterning as a whole (Hughes 2003a, b; Minelli et al. 2003).

In this article, we examine aspects of the development of segments within the trunk region of the trilobite *Hintzeia plicamarginis* n. sp. We show that during ontogeny the form of the posterior part of the trunk changed markedly with the appearance of a distinctive terminal region. We illustrate aspects of the growth dynamics of the immature caudal plate in this trilobite. Next we define and test a model for the development of the caudal plate during the anamorphic phase of growth, in which new segments appeared between molts. We

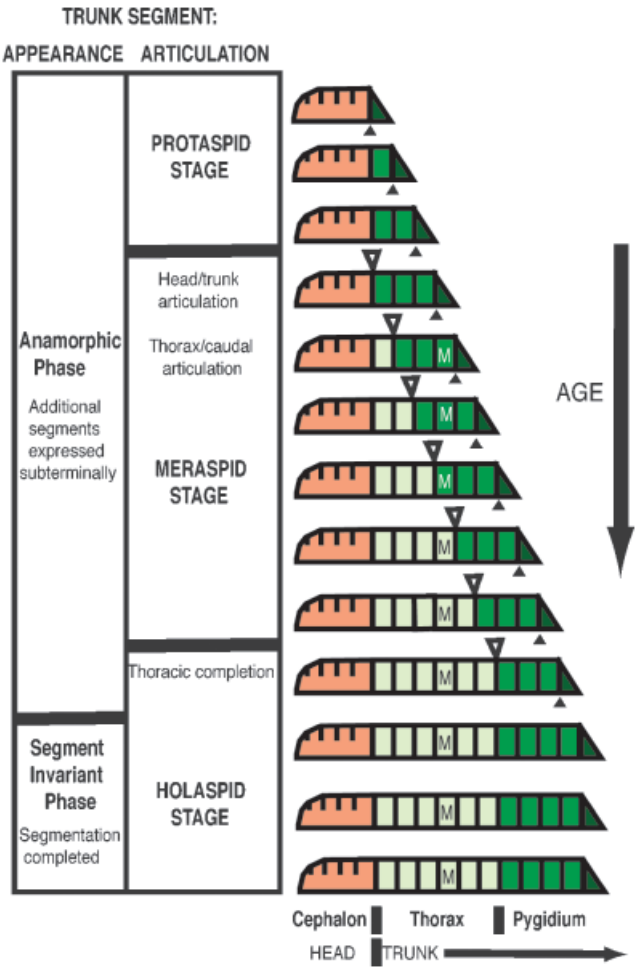

Fig. 1. Schematic representation of the ontogeny of a trilobite dorsal exoskeleton. A small solid triangle marks the place where additional segments were first expressed, a larger open triangle marks site of developing articulation. Major developmental events and stages are shown to the left. Depending on the species, the meraspid–holaspid transition could precede, coincide with or follow the anamorphosis-segment invariant phase transition. New segments are first expressed at the anterior of the posterior trunk generative zone, shown here as the dark green triangle. Conjoined trunk segments are shown in mid-tone green, freely articulating trunk segments are shown in light green. Increase in absolute size of individual segments between molts is not represented. "M" represents a distinctive segment illustrating the passage of a segment from the caudal plate into the thorax during meraspid ontogeny.

then use this model as a basis for comparing ontogenetic trajectories and calculating per segment growth coefficients for individual segments during the later stages of the development of segment articulation within the caudal plate. These results allow assessment of the degree to which segments developed as individualized entities. We show that, in general, segments destined to become thoracic segments and those destined to become the anterior of the mature caudal plate followed similar trajectories and were thus apparently homonomous in form.

TRILOBITE ONTOGENY AND THE IMPORTANCE OF *H. PLICAMARGINIS* N. SP

During the earliest fossilized phase of trilobite ontogeny, all exoskeletal segments, whether part of the cephalic or trunk regions, formed a single structure comprised of conjoined segments (Fig. 1). Successive molts were accompanied by the expression of additional trunk segments, first appearing at the anterior of a short terminal generative zone (Stubblefield 1926). In all trilobites for which ontogenetic series are well known, postembryonic development was first characterized by the anamorphic appearance of new segments, followed by a phase of growth in which no new segments were expressed in the trunk exoskeleton (Fusco et al. 2004). As new trunk segments were being expressed, so new articulations developed between segments, the first being between the cephalon and anterior trunk segment. The appearance of this articulation defines the onset of the meraspid phase. During this phase the thorax, composed of fully articulated trunk segments, was constructed via the dynamic transfer of segments from the caudal plate into the thorax as new articulations developed at the posterior of the leading segment of the caudal plate at successive molts. For some portion of meraspid growth the release of thoracic segments was accompanied by the appearance of additional trunk segments near the rear of the caudal plate. Trilobites reached the holaspid phase when the last segment was released from the anterior of the caudal plate. Growth and molting did not cease at this point, but the development of tergal articulation within the trunk was complete. The mature caudal plate is known as the trilobite pygidium.

The rates of release of anterior segments and appearance of new posterior segments during the meraspid phase were not equivalent within every species, but such decoupling of segment appearance and release has not been explored in detail to date. An informal description of the ontogeny of *H. plicamarginis* n. sp. proposed that the meraspid development of this trilobite could be divided into two phases (Fig. 2): (1) an "accumulation phase," in which the rate of accretion of segments exceeded that of the development of articulations, with the result that the number of segments in the caudal plate increased between instars (Fig. 2); (2) a "shedding phase," in which the appearance of additional segments ceased the release of anterior segments continued, reducing the number of segments in the caudal plate between instars (Kopaska-Merkel 1987). These terms were cited in the revised Treatise on Invertebrate Paleontology (Chatterton and Speyer 1997), and have been applied to the ontogenies of other trilobites (McNamara et al. 2003). Consequently, these terms became part of the lexicon of trilobite ontogeny without formal

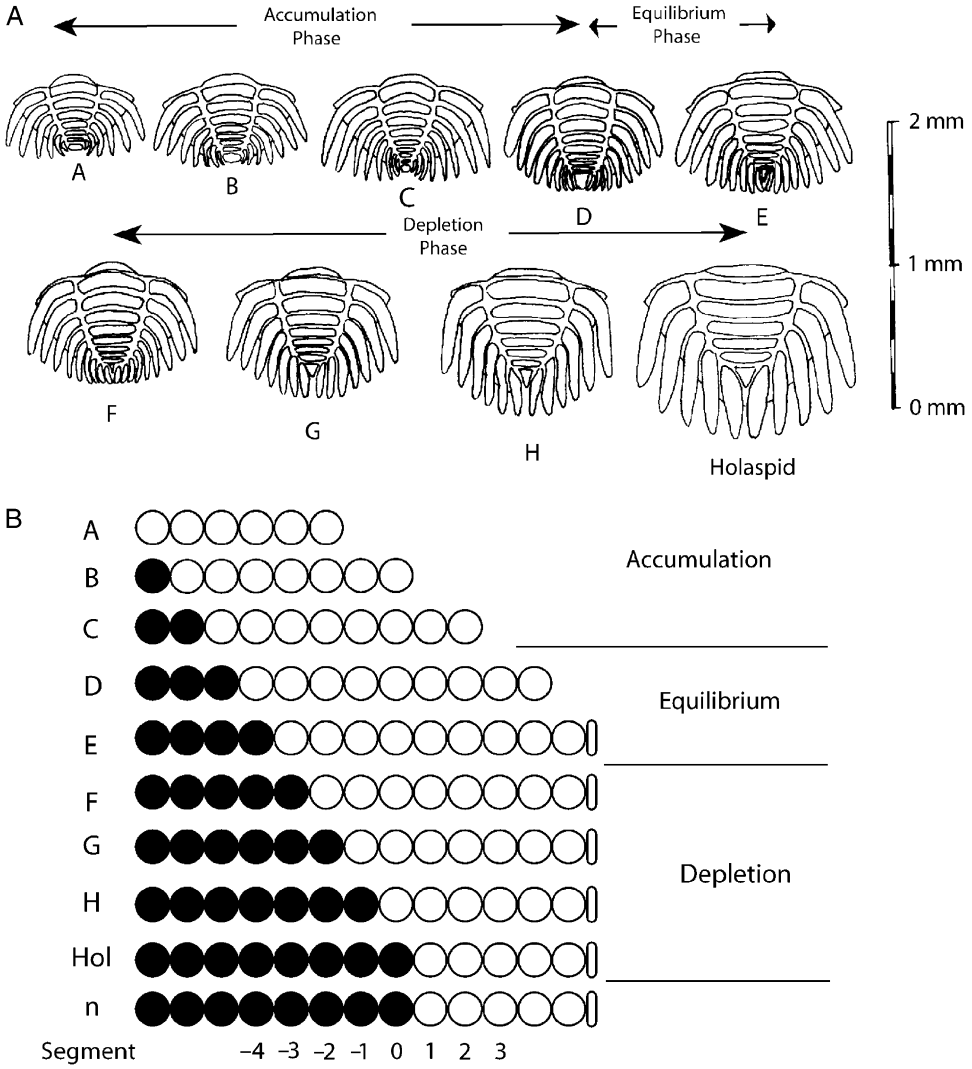

Fig. 2. The development of the caudal plate in *Hintzeia plicamarginis* n. sp. as proposed by Kopaska-Merkel (1987) and modified herein. (A) Cartoon of putative developmental stages within meraspid growth. The accumulation phase is the interval in which more segments appeared in the developing caudal plate than were released into the thorax. During the equilibrium phase the number remained constant, and during the depletion phase the number of segments declined. (B) Stylized schedule of segment accumulation and depletion within the developing caudal plate and posterior trunk region of *H. plicamarginis* n. sp. as proposed herein. (A–H) are the stages of meraspid ontogeny present within the sample. The anterior of the trilobite, not shown, is to the left. Open circles represent segments within the caudal plate, closed circles are segments hypothesized to have been released into the thorax according to the model. The lozenge-shaped structure represents the terminal piece. Note that additional thoracic segments released into the thorax before stage A may have occurred and are not shown. Anamorphic segment expression in the trunk was completed by the onset of stage (E). Hol represents the first holaspid instar, n represents any subsequent holaspid instar. Individual segments are identified as follows: Segment 0 is the posteriormost segment destined to enter the thorax. Segments posterior to segment 0 remain in the caudal plate in maturity and are given positive numbers (1, 2), whereas segments anterior to segment 0 are designated by negative numbers (-1, -2, -3, etc.).

description or documentation. In this article, we provide such information and test whether the number and sequence of instars initially proposed can be supported quantitatively. An additional phase, named the "stasis phase," in which the rate of appearance of segments was balanced by the rate of release, has recently been applied to the meraspid ontogeny of other trilobites (McNamara et al. 2003, p. 117). We suggest substitution of the term "equilibrium phase" for the name "stasis phase" because the former better reflects the dynamic balance between segment appearance and release, rather than implying a static pattern. Similarly, we propose substitution of "depletion phase" for "shedding phase" because release of segments likely occurred at all stages of meraspid growth, including the accumulation phase. "Depletion" complements "accumulation" in that both refer to trends in net segment number in the developing caudal plate.

GEOLOGIC SETTING AND ANALYTICAL PROCEDURES

All material of *H. plicamarginis* n. sp. came from a sample of light gray lime mudstone (D450-465) collected from the upper Broken Skull Formation, 121 m below the base of the Sunblood Formation at Section D, measured at 10 km east of the east branch of Natla River (63°09′ N, 127°58′ W) in the Mackenzie Mountains, District of Mackenzie, Northwest Territories, Canada (Ludvigsen 1975, Figs. 1, 7, 8). In this area, the Broken Skull Formation consists of peritidal and shallow subtidal carbonates with oncolites and wind-blown quartz sand grains (Gordey and Anderson 1993). The outer shelf margin of these carbonates is defined by a reef tract composed of coalesced mounds of thrombolites and *Renalcis* coarsely recrystallized to dolostone (Pratt 1988). The fossil-

bearing block was collected from shallow subtidal limestones about 60 m above the highest of these thrombolite mounds. Etching of the sample with dilute hydrochloric acid yielded exceedingly abundant disarticulated, finely silicified trilobites of the genera *Hintzeia*, *Pseudohystricurus, Psalikilus, Pilekia*, and *Leoforteyia* (Ludvigsen and Westrop 1986). The collection also yielded abundant conodonts characteristic of the *Acodus deltatus–Microzarkodina dianae* faunal association (Tipnis et al. 1978) that, in Utah, occur in the Ross/Hintze zones F to H in the middle Fillmore Formation (Ethington and Clark 1981). Our material comes from the Stairsian-Tulean boundary interval that is part of the Ibexian Series (Ross et al. 1997) of the Ordovician Period and is about 485 Myr old (Sadler and Cooper 2004).

Caudal plates of *H. plicamarginis* n. sp. were examined and digitally photographed under a stereoscopic light microscope. The sagittal (sag.) length and transverse (tr.) width measurements were made using a graticule by D. K.-M., and the locations in two dimensions of landmarks on the dorsal surface of the caudal plate were extracted using NIH Image software by A. G. S. Landmarks were selected for the first three segments of the caudal plate (Fig. 8). All nonaxial landmarks were reflected from one side using sagittal landmarks as a baseline, and averages were calculated for the position of each bilaterally symmetrical pair of landmarks, where possible. This permitted the inclusion of specimens in which one of the paired landmarks was not available. Landmark points were manipulated and analyzed using the IMP software package written by David Sheets of Canisius College (http://www.canisius.edu/ ~ sheets/morphsoft.html).

The program BigFix 6.0 was used to permit reflection across the baseline, and CoordGen 6.0 to generate the Procrustes shape coordinates, Bookstein shape coordinates, and centroid size estimates. DisparityBox 6.0f estimated shape variation within segments and Two Group 6.0f was used to assess the degree of shape difference between segments. Both these approaches used Procrustes shape coordinates and distances (see Hughes et al. 1999 for the use of a similar approach). VecCompare 6.0f was used to compare ontogenetic trajectories based on the Bookstein shape coordinates only (see Webster et al. 2001 and references therein). The ANOVA was performed using Systat Version 8.0. Measurement error was estimated by making multiple mountings, images, and measurements of a single specimen.

THE ONTOGENY OF THE CAUDAL PLATE OF *H. plicamarginis* N. SP

In 1987, isolated caudal plates of *H. plicamarginis* n. sp. were assigned to morphotypes based on overall size, shape, and number of segments, and arranged into a series of eight putative sequential instars (Kopaska-Merkel 1987), representing the later portion of the meraspid ontogeny of this species (Fig. 2). Kopaska-Merkel (1987) proposed that during the accumulation phase each molt was accompanied by the addition of two new segments for each segment that was released into the thorax. In the depletion phase, no additional segments appeared but the release of anterior segments persisted. This continued until a stable number of five segments within the caudal plate was reached, when the holaspid phase began. The form of the caudal plate in each of these eight stages is described below.

Stage A

The smallest caudal plates of *H. plicamarginis* n. sp. in the collection, dorso-ventrally flattened, with five clearly demarcated and one weakly developed axial rings and six pleurae with marginal spines (Fig. 3(1–3)). Pleurae divided into short (extra-sagittally [exsag.]), low propleurae with short (exsag.) pleural furrow, and inflated, rib-like opisthopleurae extending beyond margin into long spines with circular to elliptical cross section. Propleurae terminate at approximately two thirds in anterior segments to half in posterior segments of the width (tr.) of the opisthopleurae. Opisthopleurae transverse proximally, curving posteriorally in distal portion with terminal spine diverging at 25° to anterior–posterior (a–p) axis in anterior-most segment, more rearwardly directed in posterior segments. Doublure rim-like, short (tr., sag.), concave ventrally, of constant length about margin. Axis and opisthopleurae pustulose in some specimens. $n = 11$.

Stages B–D

Stage B is distinguished from stage A by the possession of one additional segment and by an increase in the size of segments apparent in the preceding stage (Fig. 3(4–7)). Stages C and D are distinguished from stage B and C, respectively, in the same ways (Fig. 4). Other progressive changes include the increasingly pendent orientation of the anterior opisthopleural spines and the slight dorsal flattening of the opisthopleurae between stages. Stage B: $n = 31$, stage C: $n = 56$, stage D: $n = 29$.

Stage E

Nine segments expressed in both axial and pleural regions as in stage D, but ninth set of pleural spines markedly more prominent and separated proximally by a small triangular terminal piece that does not extend to the posterior margin (Figs. 5(1) and 6(2)). Posterior margins of the ninth pleural spine pair conjoined distally, separated by a sagittal furrow. $n = 19$.

Stages F–H

Differing progressively from preceding stages by having one fewer segment at each stage (Fig. 5(2–4)). Pleural spines increasingly pendent posteriorly along a–p axis and between stages. Pustules no longer clear after stage F. Opisthopleural spine bases merge with doublure, which widens and flattens,

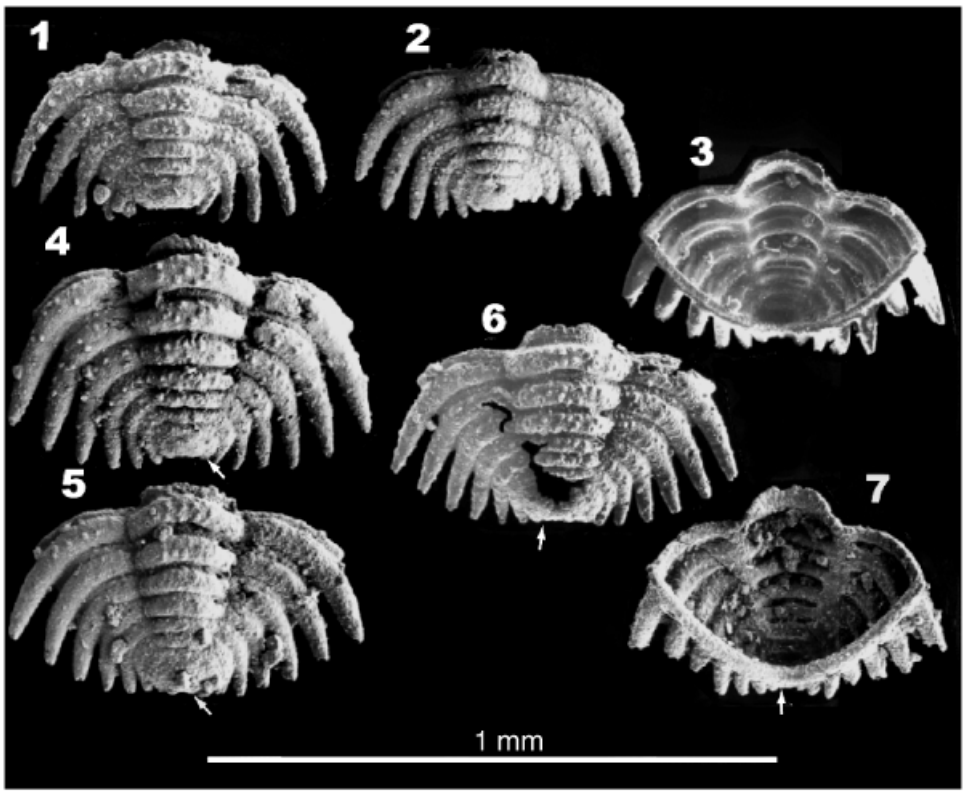

Fig. 3. Paratype meraspid caudal plates of *Hintzeia plicamarginis* n. sp. All images are scanning electron micrographs, all represent the accumulation phase. 1, stage A, dorsal view, ROM 45421; 2, stage A, dorsal view, ROM 45422; 3, stage A, ventral view, ROM 45423; 4, stage B, dorsal view, ROM 45424; 5, stage B, dorsal view, ROM 45425; 6, stage B, dorsal view, ROM 45426; 7, stage B, ventral view, ROM 45427. Arrow indicates position of mature thoracic/caudal boundary.

with triangular inner margin (Fig. 7(1)). Terminal piece becomes more prominent between stages, but maintains form established in stage E. Stage F: $n = 19$, stage G: $n = 22$, stage H: $n = 19$.

In Kopaska-Merkel's model (1987) stages A–D represent the accumulation phase, and E–H represent the depletion phase. This growth model formalized the description of the differential development of trunk segment articulation and

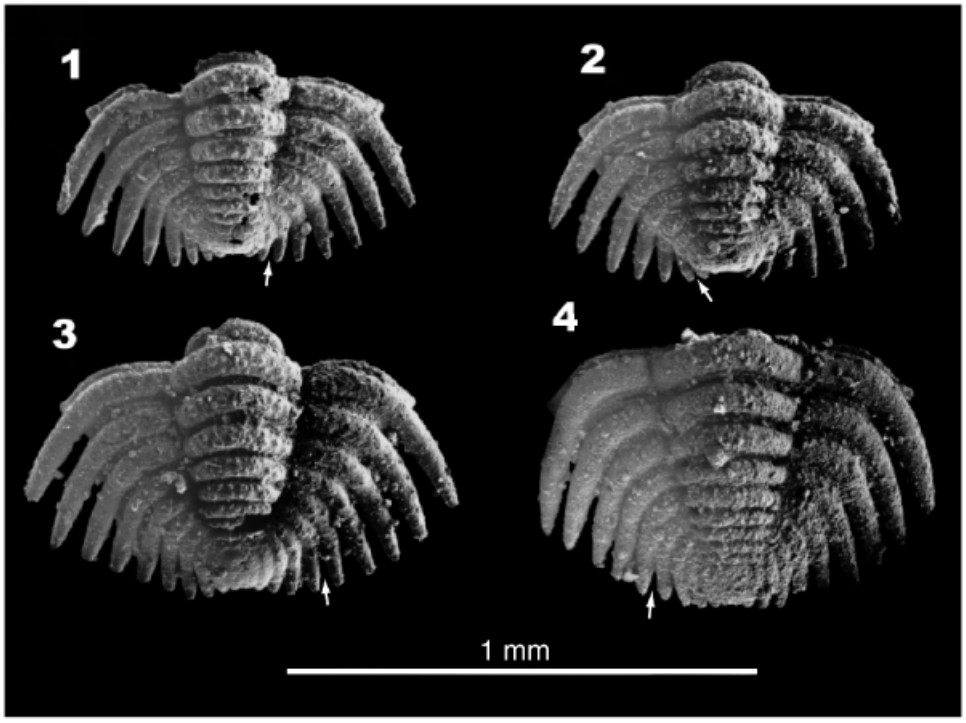

Fig. 4. Paratype meraspid caudal plates of *Hintzeia plicamarginis* n. sp. All images are scanning electron micrographs. Stage C is in the accumulation phase, stage D is in the equilibrium phase. 1, stage C, dorsal view, ROM 45428; 2, stage C, dorsal view, ROM 45429; 3, stage D, dorsal view, ROM 45430; 4, stage D, dorsal view, ROM 45431. Arrow indicates position of mature thoracic/caudal boundary.

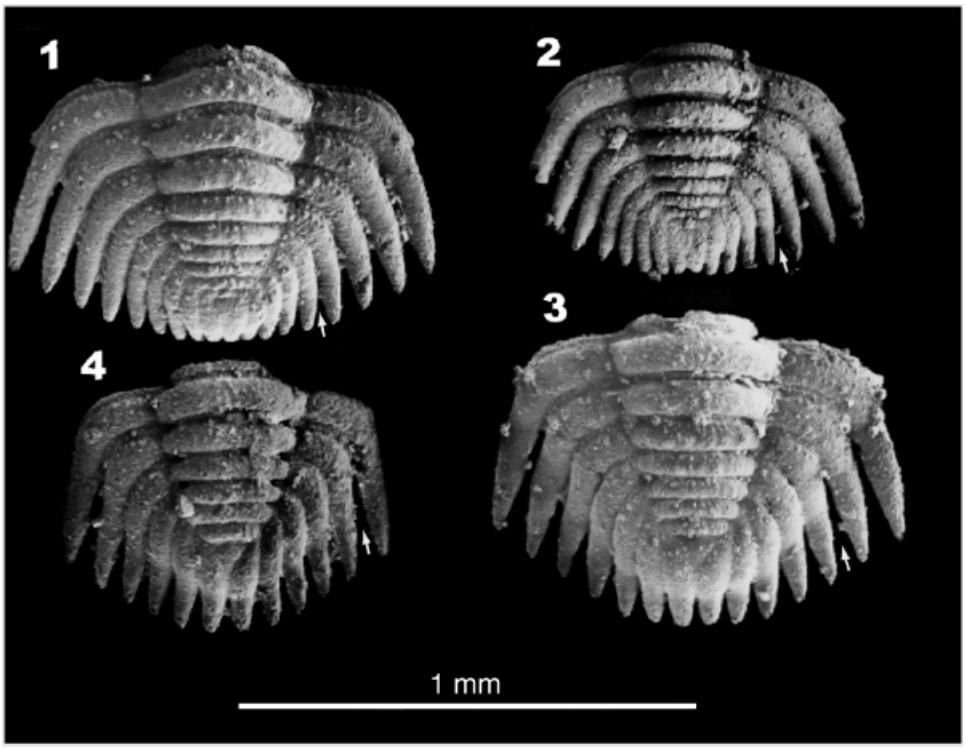

Fig. 5. Paratype meraspid caudal plates of *Hintzeia plicamarginis* n. sp. All images are scanning electron micrographs. Stage E is in the equilibrium phase, stages F–H are in the depletion phase. 1, stage E, dorsal view, ROM 45432; 2, stage F, dorsal view, ROM 45433; 3, stage G, dorsal view, ROM 45434; 4, stage H, dorsal view, ROM 45435. Arrow indicates position of mature thoracic/caudal boundary.

appearance, but it has never been tested. Alternative developmental schedules could be invoked for the same array of caudal plate morphotypes. For example, stages A and H have six, stages B and G seven, stages C and F eight, and stages D and E nine segments, respectively. If the development of segment appearance and articulation was not strictly progressive, or the sample comprised a series of polymorphs with different developmental schedules, each caudal plate morphotype might have contained more than a single instar, or the sample might have included more than one developmental pathway. Furthermore, as segments are not distinctly individualized, it is not certain that constancy in segment number within the caudal plate represents a stable complement of caudal segments rather than a precise balance between segment appearance and articulation through a series of instars. Hence it is important to test the extent to which these morphotypes, differentiated primarily on their shapes and segment numbers, differ successively in size.

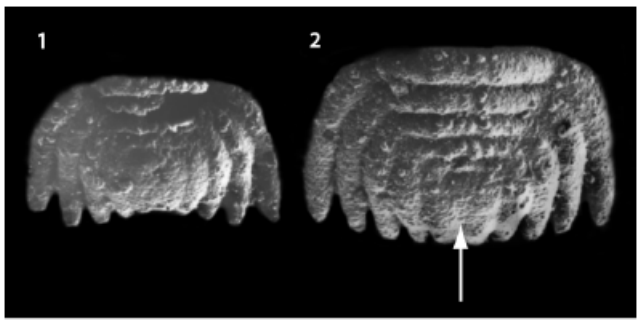

Fig. 6. The appearance of the triangular terminal piece in stage E is illustrated by the contrast between 1, stage D, ROM 45430 and 2, stage E, ROM 45432. Arrow indicates the posterior tip of the terminal piece. Only those segments that will comprise the mature caudal plate are shown.

QUANTITATIVE INVESTIGATION OF CAUDAL PLATE DEVELOPMENT

In terms of sagittal length and transverse width the caudal plate increased in size progressively up to stage E and then continued increasing in size after stage F (Figs. 8 and 9). These dimensions together provide an estimate of the "overall" size of the caudal plate. Although stages E and F are of similar size (Fig. 9A) there are clear differences in the mean size of all the other stages (Fig. 9B), and there is no indication that any of the stages contains more than a single instar. Specimens show overlap with those from other stages. The variable size increment between stages (Table 1) was apparently the result of the combination of two variables: the number of segments within the caudal plate, and the sizes of individual segments. The similar mean size of the caudal plate in stages E and F suggests that decrease in size because of the loss of one segment from the caudal plate in F compared with E, according to the Kopaska-Merkel (1987) model, was matched by the net increase in the size of the remaining segments. However, in

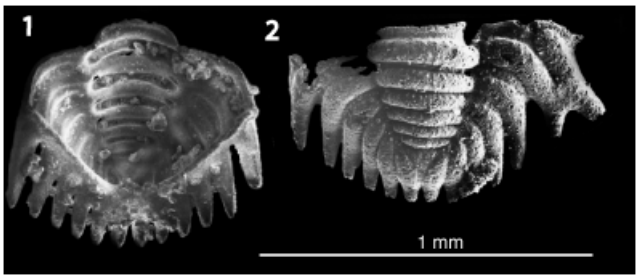

Fig. 7. Paratype meraspid caudal plates of *Hintzeia plicamarginis* n. sp. 1, stage H, ventral view, ROM 45436 and 2, stage H, dorsal view, ROM 45437, showing segmental teratology on right anterior pleurae.

stages G and H increase in the size of remaining segments more than compensated for size decreased because of the loss of segments from the anterior margin.

We conducted additional analysis on the size and shape of individual segments independently of the total number of segments in the caudal plate. A two-way analysis of variance (ANOVA) was used to test the sizes of individual segments as a function of (1) the position of a segment relative to the anterior margin of the caudal plate, (2) the putative stage assigned by Kopaska-Merkel to the specimen containing the given segment, and (3) interaction between factors (1) and (2). In the first case we asked the question whether the pattern of size differences among segments was consistent among stages, and in the second whether size differences between stages was consistent among segments. We used centroid size, the square root of the summed squared distances of all landmarks from the centroid of that array (Bookstein 1991), as an estimator of segment size. Data was extracted for the leading three segments in each putative instar between stages D–H, for which the sample size of each stage was adequate (Fig. 8).

The ANOVA results show strong statistical support for both factors ($P = 1.81 \times 10^{-11}$ between segment size and molt, and $P = 1.47 \times 10^{-11}$ between segment size and segment position). However, there is statistical support against any additional effect on centroid size because of interaction between segment position and meraspid stage ($P = 0.975$). From these results, we conclude that the size of an individual segment, defined with respect to the anterior of the caudal plate, increased both with its distance from the posterior of the caudal plate and with the stage to which it has been assigned. We can also conclude that the relative sizes of the three anterior segments of the caudal plate remained constant among the putative stages. Stages D–H show significant increase in the mean sizes of first three segments (Fig. 10) such that mean segment size increased between successive stages as

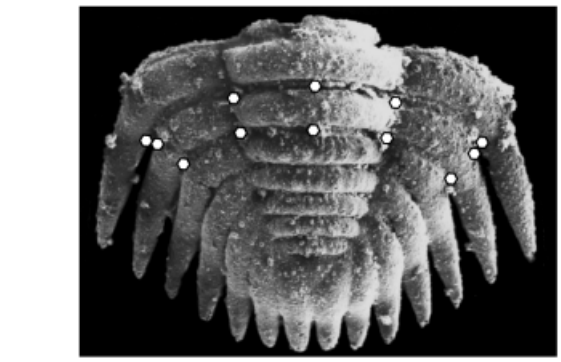

Fig. 8. Position of landmarks on a single segment measured for morphometric analysis. Data was collected from each of the first three segments of each individual. The dataset included two axial landmarks and five paired off-axial landmarks. Image is based on ROM 45434, pictured in Fig. 5 (3, stage G).

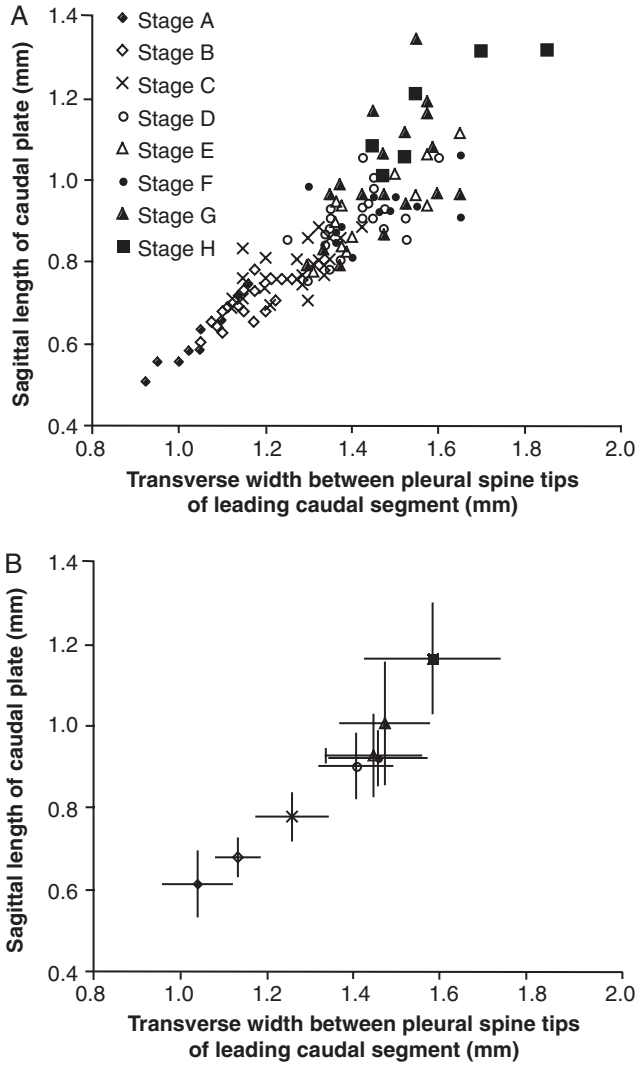

Fig. 9. The relationship between the developmental stages proposed herein and the size of the caudal plate based on all specimens available to Kopaska-Merkel (1987). (A) Individual specimens. (B) The mean scores for each stage and bars extending to one standard deviation either side of the mean.

Table 1. Growth coefficients estimated as the ratio between the mean value for a stage divided by the mean value for the preceding stage, using the transverse width between the tips of the pleural spines of the leading caudal segments and the sagittal length of the caudal plate between meraspid stages

Stage transitions	Transverse width (mm)	Sagittal length (mm)
A–B	1.09	1.11
B–C	1.11	1.15
C–D	1.12	1.16
D–E	1.03	1.03
E–F	1.01	0.99
F–G	1.01	1.09
G–H	1.07	1.16

the total number of segments in the caudal plate decreased between most of these stages. These results support the sequence of stages outlined in the Kopaska-Merkel model. Although the standard deviations in segment size vary between individual segments and stages (Table 2), the pattern is not systematic among segments. As the standard deviation of the first three segments of stage F is similar to that of a single specimen of that stage that was measured 11 times much of the apparent variation in the sizes of individual segments within stages could represent errors associated with calibration. The standard deviation within the error of size estimate within a stage is about 40% of the mean difference in size between segments, and segments in the sample of 11 measurements differ significantly in size. The apparently consistent per segment growth rate estimates for stages D–H (Table 2) support data from the growth of the caudal plate (Fig. 9) that indicates that each stage likely contained one instar.

Subsequent analyses build on these results, and assume that stages D–H are in the correct order. This model permits investigation of the fates of individual segments as the boundary between articulating and conjoined trunk segments approached them. For example, a segment third from the anterior of the caudal shield in stage D would have become the first caudal segment in stage F, and would have been released into the thorax by stage G (see Fig. 2B). By tracking the fate of individual segments between molts, we explored a variety of aspects of trunk segment development.

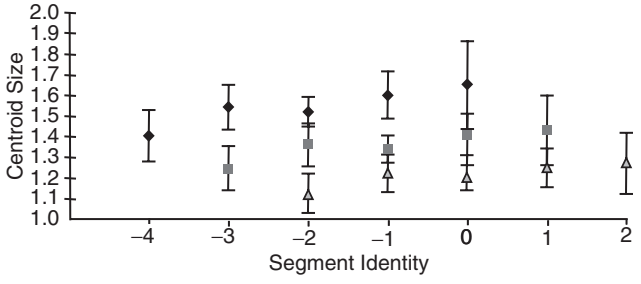

Fig. 10. Centroid size of individual segments as a function of position in the caudal plate in stages D–H. Segments at the anterior of the caudal plate are labeled as black diamonds; segments in second from the anterior as dark gray squares; segments third from the anterior as light gray triangles. Bars represent one standard deviation from the mean.

Growth ratios per segment were estimated by the ratio of the mean size of a segment between succeeding instars, according to the model of growth presented above (Table 2). These suggest an average increase in size per segment of about 1.1–1.2 per instar during the later part of meraspid ontogeny. The values derived from different segments and different instars are quite consistent, and do not appear to indicate marked changes in per segment growth increment between molts. These values are also consistent with the growth increments recorded in other trilobites (see Fusco et al. 2004). These values are broadly comparable with growth increments based on the size of the caudal plate (Fig. 9, Table 1), but are slightly higher.

We also examined the shape of individual segments during late meraspid ontogeny, and of different segments when occupying analogous positions with respect to the boundary between articulating and conjoined trunk segments. Estimates of error in shape assessment using 11 measures of a single specimen indicate that the average shape disparity per segment in the control specimen is on average 54% of the same segment at the same stage in the sample as a whole. This suggests that error may account for more than half the apparent variance in the shape of individual segments within the sample. Within the entire sample comparisons of the shapes of adjacent segments within the same stage indicate significant differences in shape in 5 out of 15 comparisons at the 95% confidence level with the Bonferroni correction applied to take into account multiple pairwise comparisons (Table 3(A)). Out of the eight comparisons of the shapes of individual segments at adjacent developmental stages four are significantly different at the 95% confidence level (Table 3(B)). There is no consistent pattern in the occurrence of these differences with respect to position within the caudal shield or segment identity. We conclude that caudal segments varied their shapes during ontogeny but that these differences were relatively subtle (see Figs. 4–6) and were frequently masked by variation within individual stages and/or measurement error. Variance in the shape of individual segments at each position showed similar mean values and overlap in the 95% confidence intervals for 14 out of 15 positions, suggesting comparable levels of variability among segments at all stages (Table 3(D)).

Comparison of the shape of different segments when occupying analogous positions with respect to the boundary between articulated and conjoined segments revealed significant differences in 3 out of 12 cases at the 95% confidence level, and in most cases different segments in analogous

Table 2. Centroid size averages (Average), standard deviations and per segment growth coefficients of individual segments relative to their position in the caudal plate with respect to the thoracic/caudal boundary (first, second, etc.)

Average	Seg 2	Seg 1	Seg 0	Seg −1	Seg −2	Seg −3	Seg −4
First			1.64	1.60	1.51	1.54	1.40
Second		1.43	1.41	1.33	1.36	1.24	
Third	1.27	1.25	1.19	1.22	1.12		
Standard Deviation	Seg 2	Seg 1	Seg 0	Seg −1	Seg −2	Seg −3	Seg −4
First			0.21	0.11	0.07	0.11	0.12
Second		0.17	0.10	0.07	0.10	0.11	
Third	0.15	0.09	0.06	0.09	0.09		
Growth coefficient		Seg 1	Seg 0	Seg −1	Seg −2	Seg −3	
2nd–1st			1.18	1.09	1.22	1.24	
3rd–2nd		1.14	1.17	1.20	1.11		

Individual segments are identified (Seg 2, Seg 1 etc.) following the convention established in Fig. 2B.

positions were apparently more similar than those of the same segment at adjacent stages (Table 3(C)). Highly significant shape differences occurred in the shapes of segments 0 and 1 both when in the second and third positions with respect to the boundary between articulated and conjoined segments. This might suggest that during late meraspid ontogeny there was a notable difference in form between the last segment that would have been released into thorax, and the leading segment of the mature caudal shield (Table 3(C)). However, there is another highly significant difference between segments in the second from anterior position (segments −2 and −1) between stages E and F that is not apparent at either the previous or subsequent stage.

To assess the pattern of shape change during ontogeny, vectors of shape change were calculated for individual segments between adjacent stages (see above for details of programs and methods used). These were compared with vectors between other stages for the same individual segments, and with those of different segments as they assumed analogous positions with respect to the boundary between articulated and conjoined segments (Table 4). In 13 out of 15 comparisons the magnitude of differences between vectors of shape change lay within the 95% confidence limits based on bootstrapped resampling. The two significant differences both related to segment–1 during its transition from third- to second-most anterior segment in the caudal plate in stages E to F but do not appear related to a marked or unusual change in shape (Fig. 5(1 and 2)), nor is the degree of shape variance associated with either of these stages apparently anomalous (Table 3D). Hence our analysis did not detect consistent, significant differences in patterns of growth for individual segments between stages or between different segments when assuming similar positions with respect to the boundary between articulated and conjoined segments.

DISCUSSION

Analyses of caudal plate dimensions and the size of leading segments within it suggest that the sample is best interpreted as an ordered sequence of stages, each of which likely represents one instar. Although adjacent segments differed in shape in some cases and ontogenetic changes in shape were evident through this series (Figs. 3–7), the magnitude of shape change per molt was relatively small and the pattern of shape change appears to have been relatively consistent among trunk segments. Segment growth increments per instar are comparable with those known in other trilobites (Fusco et al. 2004). Our results indicate that the order of stages proposed by Kopaska-Merkel (1987) is applicable to the equilibrium and depletion phases of meraspid caudal plate ontogeny. Moreover, the stage D–E transition appears to coincide with the appearance of the mature terminal piece. Therefore, the stage D–E transition represents an equilibrium phase in terms of segment numbers (excluding the terminal piece) that spans a single molt, set between accumulation and depletion phases.

The manifestation of a distinct terminal piece in stage E need not represent the first appearance of a post segmental region, as such was apparent in earlier stages (Figs. 3(4 and 6) and 4). Hence, we do not consider the terminal piece as the last of a series of trunk segments, but as a distinct exoskeletal morphology manifest at the completion of segment accretion (Fig. 2B).

We are unable to test Kopaska-Merkel's (1987) view that the accumulation phase consisted of the release from the developing caudal plate of two segments for every one added because of the absence of articulated material in which the development of the thorax can be observed directly. Other possible developmental schedules include onset of the release of thoracic segments coincident with the start of the depletion phase, as may have been the case in some cheirurids (Whit-

Table 3. Statistical analysis of shape variance within and between segments

Position (A)	D	E	F	G	H
1–2	0.390	0.003	0.003	0.058	0.010
2–3	0.830	0.193	0.003	0.245	0.015
1–3	0.440	0.003	0.003	0.010	0.010

Segment (B)	1	0	− 1	− 2	− 3
2–1		0.002	0.047	0.002	0.135
3–2	0.002	0.297	0.002	0.725	

Position (C)	D–E	E–F	F–G	G–H
1	0.728	0.108	0.099	0.555
2	0.455	0.002	0.113	0.001
3	0.400	0.109	0.002	0.616

Segment/Measurement (D)	D	E	F	G	H
2					0.007
2 (95% lr)					0.004
2 (95% up)					0.008
1				0.009	0.009
1 (95% lr)				0.003	0.003
1 (95% up)				0.015	0.013
0			0.004	0.009	0.008
0 (95% lr)			0.003	0.003	0.003
0 (95% up)			0.005	0.015	0.010
− 1		0.003	0.007	0.006	
− 1(95% lr)		0.002	0.003	0.004	
− 1 (95% up)		0.004	0.009	0.165	
− 2	0.007	0.004	0.007		
− 2 (95% lr)	0.002	0.002	0.003		
− 2 (95% up)	0.179	0.005	0.010		
− 3	0.071	0.004			
− 3 (95% lr)	0.002	0.002			
− 3 (95% up)	0.247	0.005			
− 4	0.052				
− 4 (95% lr)	0.002				
− 4 (95% up)	0.137				

(A) *P* values for the significance of shape differences in pairwise comparisons among segments within stages, based on the Procrustes distance between segments. Stages are columns, rows are comparisons between segments occupying different positions relative to the anterior margin of the caudal plate. The threshold value for significance at the 95% confidence level based on Bonferroni correction is 0.003. (B) *P* values for shape difference in the same segment when occupying different positions relative to the anterior margin of the caudal plate (and therefore at different stages). The identity of individual segments is given in the columns, the positions being compared with respect to the anterior margin of the caudal plate are given in the rows. The threshold value for significance at the 95% confidence level based on Bonferroni correction is 0.004. (C) The shape of segments in analogous positions relative to the anterior margin at different stages. Stages are columns, positions with respect to the anterior margin of the caudal plate are rows. The threshold value for significance at the 95% confidence level based on Bonferroni correction is 0.006. (D) The shape variance for each of the first three segments at each of the first three positions with respect to the anterior margin of the caudal plate in stages D–H. Stages are columns, rows are segments identified as in the caption of Fig. 2B. Ninety-five percent lr and up represent the lower and upper 95% confidence intervals of the shape variance based on 400 bootstrap resamples.

tington and Evitt 1953), or one or more molts during the accumulation phase in which thoracic segments were not released. These alternative explanations seem unlikely because they apparently would result in a mature thorax with an unusually low segment count for a pliomerid trilobite, which normally had between 11 and 19 segments at maturity (Henningsmoen 1959, p. O439). It is also possible that the advent of a stable number of caudal segments following the depletion phase marked transition to a second equilibrium phase. However, the sagittal length of the caudal plate at the apparent onset of the holaspid phase was about 0.65 mm, which is comparable with that of the first holaspid pygidium in other pliomerid trilobites (Lee and Chatterton 1997). Nevertheless, a wide variety of scenarios for trunk construction could be postulated in the absence of information on the development of the thorax.

The extent to which the mature caudal plate in trilobites constitutes a distinct tagma is currently debated (Hughes 2003a, b; Minelli et al. 2003). In some trilobites there was a profound difference between the morphology of segments in

Table 4. Comparisons of patterns of shape change at different stages of the ontogeny of individual segments and as different segments occupied analogous transitions with respect to the anterior of the caudal plate

Segment	0	− 1	− 2
3–2/2–1 positions	34.7	71.8	35.8
3–2 var.	72.1	31.9	108.3
2–1 var.	114.2	56.7	142.1
2–1	Seg 0	Seg – 1	Seg – 2
Seg – 1	27.1		
Row variation	63.4		
Column variation	119.6		
Seg − 2	33	38.7	
Row variation	149.2	143.7	
Column variation	116.5	116.5	
Seg – 3	32.8	14.3	45.1
Row variation	62.5	53.4	50
Column variation	114.9	55.3	146.8
3–2	Seg 1	Seg 0	Seg − 1
Seg 0	81.4		
Row variation	70.1		
Column variation	86.1		
Seg – 1	106.7	46	
Row variation	37	33.7	
Column variation	93.6	64.4	
Seg − 2	107.6	35.4	52.3
Row variation	113.8	117.5	110.4
Column variation	88.1	65.1	32.2

The upper part of the table compares the pattern of shape change as individual segments transitioned from being the third to the second segment within the caudal plate with that as they transitioned from being the second to the first segment in the caudal plate. Segments are identified as in the caption of Fig. 2B. The value given is an angle that expresses the degree of difference in the ontogenetic trajectories compared. Values marked "Var" are estimates of the within group variance of this angle for each ontogenetic transition based on 400 bootstrap resamplings of group membership. If either of these within-group values exceeded the angle between groups then the trajectories are statistically indistinguishable at the 95% confidence level. The lower part of the table uses the same approach to compare the trajectories of different segments as they transitioned through analogous positions with respect to the anterior of the caudal plate. "Row variation" refers to the segment specified in the row immediately above, "column variation" refers to the segment in the column. Results for the transition from the second to the first segment position in the caudal plate (2–1 pools) are given above those for the transition from the third to the second position (3–2 pools).

the mature thorax and pygidium (labeled the heteronomous or "two batch" trunk segment condition by Hughes 2003a, b), but in others all trunk segments are similar in form, with those of the mature pygidium differing only in lacking articulating sutures between segments (termed the homonomous trunk segment condition). The results of this analysis suggest that within the caudal plate of *H. plicamarginis* n. sp. there was no marked difference during later meraspid growth in either the shape or growth trajectory of segments destined to become part of the thorax from those destined to become part of the mature caudal plate. This is consistent with the notion of an homonomous transition in segment morphology across the mature thoracic/pygidial divide in this trilobite.

We interpret the anterior margin of the terminal piece of *H. plicamarginis* n. sp. to equate to the "pygidial biramous–terminal" boundary in the generalized model of trilobite anterior-posterior patterning presented by Hughes (2003a, Fig. 5). The appearance of the terminal piece as a distinct entity in stage E may reflect the transition from a mode of anamorphic growth in which the subterminal generative zone was dedicated to building additional segments to the later, segment invariant phase during which segments built previously grew but no new trunk segments were added (see Fusco et al. 2004).

SYSTEMATIC PALEONTOLOGY

Class Trilobita Walch 1771
Order Phacopida Salter 1864
Suborder Cheirurina Harrington and Leanza 1957
Family Pliomeridae Raymond 1913
Subfamily Cybelopsinae Fortey 1979; emended Lee and Chatterton 1997
Genus *Hintzeia* Harrington 1957

Type species: *Protopliomerops aemula* Hintze 1953

Diagnosis: Anterior cranidial border reflexed posterodorsally over frontal glabellar lobe in the holaspid phase; hypostomal middle lateral spines near posterolateral corners; L1 larger than L2 or L3; palpebral lobes opposite S2; S3 anterior or posterior to anterolateral glabellar corners; palpebral lobes medium-sized and not protuberant; pygidium of 5 axial and pleural segments with small, triangular terminal piece; pygidial pleural spines subparallel to exsagittal line or slightly divergent distally.

Discussion: The distinctive retroflexed anterior border and larger L1 may provide synapomorphies for *Hintzeia,* as may the position of the hypostomal spines, although this condition is variable within *H. plicamarginis* n. sp. *Protopliomerops celsaora* is removed from *Hintzeia*. The similarities of *P. celsaora* to *H. aemula* were discussed by Demeter (1973), who suggested that the two species as diagnosed by Ross (1951) and Hintze (1953) were the endpoints of a continuous range of morphologies, a conclusion not supported by examination of the type material upon which he based his conclusion. The similarities between the two species are here interpreted as resulting from their positions near the stems of their respective groups. *H. glabella* Kobayashi 1960 does not belong in this genus because it lacks the distinctive upturned cranidial border. The hypostome and pygidium are unknown, and so the phylogenetic position of this species cannot be properly evaluated at this time.

Species referred to *Hintzeia*: *Protopliomerops aemula* Hintze, *Protopliomerops firmimarginis* Hintze, *Hintzeia plicamarginis* n. sp.

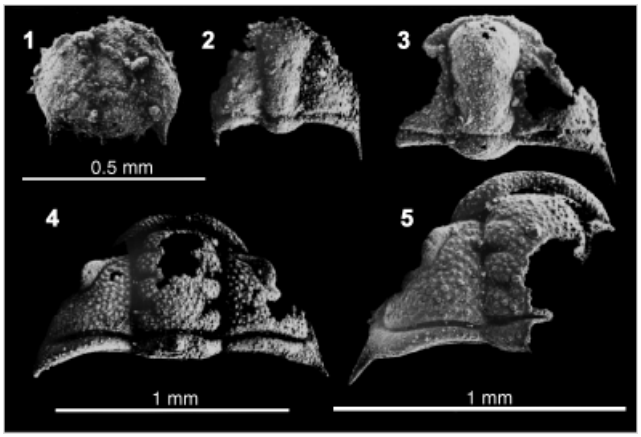

Fig. 11. Protaspid dorsal exoskeleton, possibly of *Hintzeia plicamarginis*, and meraspid and early holaspid cranidia assigned to *H. plicamarginis* n. sp. 1, Protaspid, dorsal view, ROM 45443. Left anterior margin broken; 2–3, small meraspid cranidia, scale as for 1; 2, dorsal view, ROM 45444; 3, dorsal view, ROM 45445; 4–5, late meraspid or early holaspid cranidia; 4, dorsal view, ROM 45646; 5, dorsal view, ROM 45447. Note incipient upturn of anterior border.

Hintzeia plicamarginis n. sp.
(Figs. 3–7 and 11–14)
1987 *Hintzeia* n. sp. Kopaska-Merkel, p. 43–44.

Diagnosis: Pygidial spines relatively short and stout, pleural ribs bent dorsally at or just distal to point where they become free spines; cranidium triangular, anterior margin forms blunt point medially; three pairs of hypostomal marginal lateral spines sharp, outwardly directed; bulbous projection of central body of hypostome reaches or overhangs anterior hypostomal border (ventral view).

Holotype: Holaspid cranidium, ROM 45466 (Fig. 14(3–5)).

Repository: All type and figured specimens deposited in the invertebrate paleontology collections of the Royal Ontario Museum, Toronto, numbers ROM 45421–45435, 45443–45469.

Etymology: Latin, *plico*, fold, and *margo*, border, in reference to the prominent upturned anterior cranidial border.

Description: Anterior cranidial border folded back to form shelf over preglabellar furrow and part of the frontal glabellar lobe; shelf bears posteromedial semicircular indentation flanked by two blunt projections; glabella slightly tapered anteriorly; S1–S3 furrows deep, angled posteromedially, L1–L3 approximately equal in size (exsag., tr.); L1 lobes nearly isolated by sharply curved S1 furrows. SO entire, shallowing medially. Small cranidia bear small mesial occipital node on short (exsag.) LO. Palpebral lobe anterior opposite L3, posterior opposite L2; distinct, broader and more elevated than ocular ridges, palpebral furrow shallow, ocular ridges bounded anteriorly and posteriorly by slope changes without distinct furrows. Posterior course of facial suture in dorsal view gently convex outward, only slightly more outwardly directed than anterior course, so that cranidium forms equilateral triangle without major indentations for librigenae (which were nearly vertical in life). Small spinule present at genal angle in some specimens. Entire exoskeleton covered with fine granules; fixigenae finely pitted.

Hypostome bears three pairs of lateral marginal spines. Anterior pair occurs at about mid-length (exsag.) of hypostome, and posterior pair at about posterolateral corners, but middle pair may be equidistant between the other two or so close to the posterior pair that their bases nearly touch. Posterior margin medially pointed or produced into blunt spine. Lateral border narrow (tr.), posterior border moderately broad (sag., tr.) and flat.

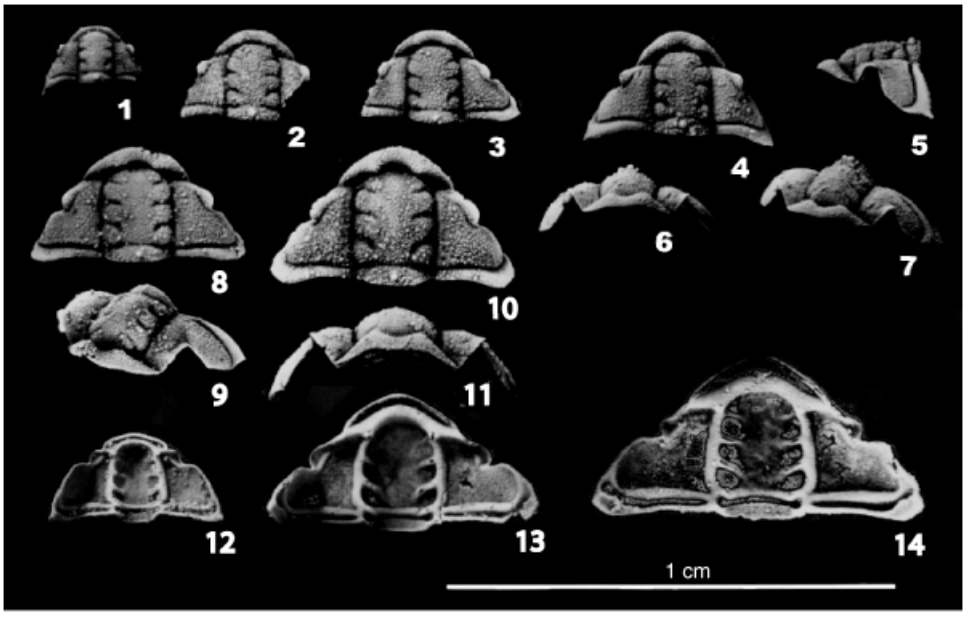

Fig. 12. Large meraspid or small holaspid cranidia of *Hintzeia plicamarginis,* n. sp. 1, dorsal view, ROM 45448; 2, dorsal view, ROM 45449; 3, dorsal view, ROM 45450; 4–7, ROM 45451; 4, dorsal view; 5, lateral view; 6, anterior view; 7, oblique anterodorsal view; 8–9, ROM 45452; 8, dorsal view; 9, oblique anteriodorsal view; 10–11, ROM 45453; 10, dorsal view; 11, anterior view; 12, ventral view, ROM 45454; 13, ventral view, ROM 45455; 14, ventral view, ROM 45456.

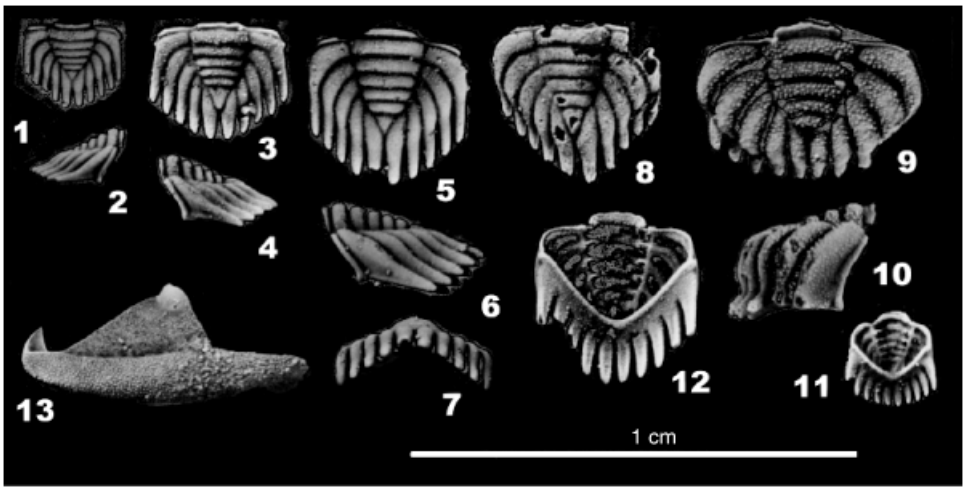

Fig. 13. Librigena and small holaspid pygidia of *Hintzeia plicamarginis* n. sp. 1–11. Pygidia. 1–2, ROM 45457; 1, dorsal view; 2, lateral view; 3–4, ROM 45458; 3, dorsal view; 4, lateral view; 5–6, ROM 45459; 5, dorsal view; 6, lateral view; 7–8, ROM 45460; 7, lateral view; 8, dorsal view; 9–10, ROM 45461; 9, dorsal view. Note unusual morphology which might be interpreted as a rare species closely allied to *H. plicamarginis*. 10, lateral view; 11, ventral view, ROM 45462; 12, ventral view, ROM 45463; 13, librigena, lateral view, ROM 45464.

Librigenal ocular platform small and triangular; posterior margin nearly normal to marginal furrow.

Pygidial axis of five segments (invariant in 57 holaspid pygidia, and dozens of broken specimens with countable spines) and small triangular terminal piece, sagittal length of terminal piece 1/4 to 2/5 that of posterior pair of pleura in plan view; pleura composed of five pairs of blunt tubular spines distally; spines pendent in dorsal view with little or no posterolateral divergence; spines bent dorsally at or just distal to point where they become free of pleura; in lateral view this bend is seen as a concave-up inflection two thirds of distance from dorsal furrow to spine tip; doublure narrow (sag., tr.), of constant width, with rim projecting ventrally, bears small hollow bosses anteriorly, which probably articulated with last thoracic segment.

Ontogeny: Associated metaprotaspid about 0.3 mm in length with three pairs of protocranidial spines and two pairs of protopygidial spines, but it is possible that protaspid belongs to the species of *Pilekia* recovered from this fauna. Early meraspid cranidia with glabella clavate and prominent rearward directed genal spine, the relative length (exsag.) of which decreases during meraspid ontogeny and becomes obsolete. Meraspid ontogeny accompanied by relative widening of the posterior glabellar lobes to form a straight-sided glabella in maturity. Cranidal anterior margin may develop from thin band in associated protaspids, lengthening (sag.) and inflating with the development of two prominent inflections along its posterior margin that extend toward the abaxial portions of L4, sagittal portion of posterior margin bowed anteriorly. Occipital node, prominent in early meraspids.

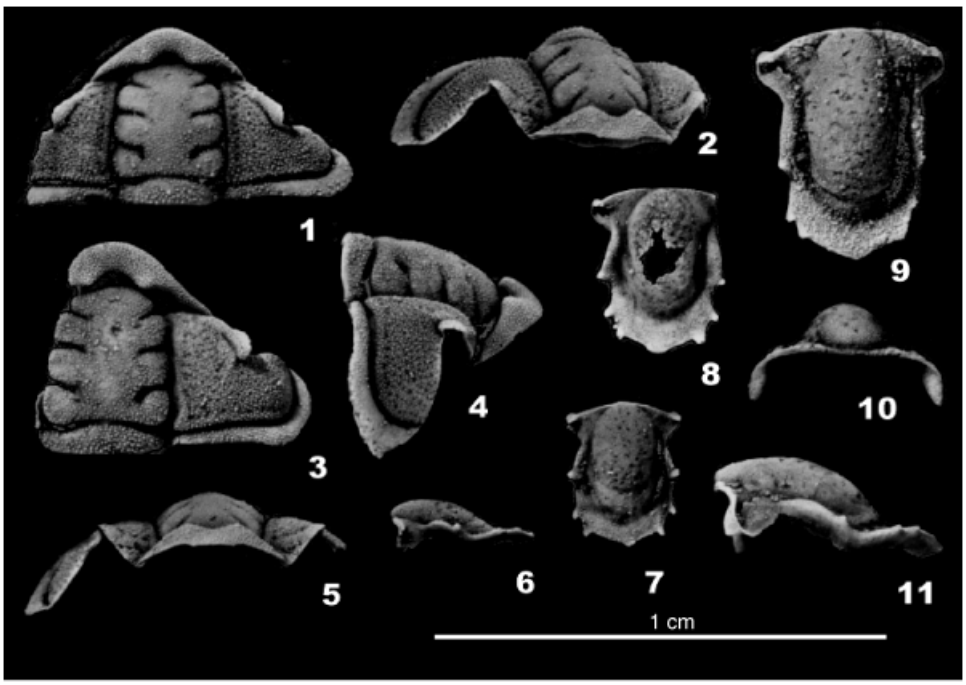

Fig. 14. Hypostomes and likley holaspid cranidia of *Hintzeia plicamarginis* n. sp. 1–5, Cranidia; 1–2, ROM 45465; 1, dorsal view; 2, oblique anterodorsal view; 3–5, Holotype, ROM 45466; 3, dorsal view; 4, lateral view; 5, anterior view; 6–10, Hypostomes; 6–7, ROM 45467; 6, lateral view; 7, ventral view; 8, ventral view, ROM 45468; 9, ventral view, ROM 45469. Note variation in size, orientation, and placement of marginal spines. 10–11, ROM 45469; 10, anterior view; 11, lateral view.

Discussion: *Hintzeia plicamarginis* most closely resembles *H. firmimarginis*, differing primarily in having shorter and stouter pygidial spines bent dorsally rather than straight; longer hypostomal lateral marginal spines, more outwardly directed anterior hypostomal margin (in ventral view), cranidium more nearly triangular in dorsal view and more pointed anteriorly (only in large mature forms); eyes situated more anteriorly and more laterally; pygidial doublure of *H. firmimarginis* bears minute lobe projecting anterodorsally along axis; librigenae indistinguishable. *H. plicamarginis* is readily distinguished from *H. aemula* on the basis of the folded and invaginated anterior cranidial border.

Acknowledgments

Our Ordovician trilobite studies are supported by the donors of the American Chemical Society Petroleum Research Fund through grant ACS PRF#39915-AC8, which we gratefully acknowledge. Publication was facilitated by grant USP-S-04-004 from the NASA Exobiology program. We thank Richard A. Fortey and Mark Webster for detailed, constructive reviews, and Mary L. Droser and Peter M. Sadler for additional comments. R. L. acknowledges the assistance of David G. Perry in collecting these rich samples under difficult circumstances. Their joint fieldwork in the Mackenzie Mountains in 1973 was supported by the Geological Survey of Canada. David died 25 years ago in a helicopter crash in western Alberta. D. K.-M. acknowledges R. L. for postdoctoral support. We thank David Sheets for making the software freely available to us, and James Bryant, Douglas Haywick, Andrew Rindsberg, and Janet Waddington for making materials available to us. David M. Robinson and Adrian Rushton provided helpful suggestions on terminology.

REFERENCES

Bookstein, F. L. 1991. *Morphometric Tools for Landmark Data*. Cambridge University Press, New York.

Chatterton, B. D. E., and Speyer, S. E. 1997. Ontogeny. In H. B. Whittington (ed.). *Treatise on Invertebrate Paleontology, Part O, Arthropoda 1. Trilobita, Revised*. Geological Society of America and University of Kansas, Boulder and Lawrence, pp. 173–247.

Cisne, J. L., Chandlee, G. O., Rabe, B. D., and Cohen, J. A. 1980. Geographic variation and episodic evolution in an Ordovician trilobite. *Science* 209: 925–927.

Cotton, T. J., and Braddy, S. J. 2004. The phylogeny of arachnomorph arthropods and the origin of the Chelicerata. *Trans. Roy. Soc. Edinburgh-Earth Sci.* 94 (for 2003): 169–193.

Demeter, E. J. 1973. Lower Ordovician pliomerid trilobites from western Utah *Brigham Young Univ. Geol. Stud.* 20: 37–65.

Ethington, R. L., and Clark, D. L. 1981. Lower and Middle Ordovician conodonts from the Ibex area, western Millard Co., Utah. *Brigham Young Univ. Geol. Stud.* 28: 1–155.

Fortey, R. A. 1979. Early Ordovician trilobites from the Catoche Formation (St. George Group), Western Newfoundland. *Bull.-Geol. Surv. Can.* 321: 61–114.

Fortey, R. A., and Owens, R. M. 1991. A trilobite fauna from the highest Shineton Shales in Shropshire, and the correlation of the latest Tremadoc. *Geol. Mag.* 128: 437–464.

Fusco, G., Hughes, N. C., Webster, M., and Minelli, A. 2004. Exploring developmental modes in a fossil arthropod: growth and trunk segmentation of the trilobite *Aulacopleura konincki*. *Am. Nat.* 163: 167–183.

Gordey, S. P., and Anderson, R. G. 1993. Evolution of the northern Cordilleran Miogeocline, Nahanni Map Area (105I), Yukon and Northwest Territories. *Geol. Surv. Canada Mem.* 428: 1–214.

Harrington, H. J. 1957. Notes on new genera of Pliomeridae (Trilobita). *J. Paleontol.* 31: 811–812.

Harrington, H. J., and Leanza, A. F. 1957. Ordovician trilobites of Argentina. *Spec. Pub. Dept. Geol., Univ. Kansas* 1: 1–276.

Henningsmoen, G. 1959. Order Phacopida. In R. C. Moore (ed.). *Treatise on Invertebrate Paleontology, Part O, Arthropoda 1. Trilobita*. University of Kansas, Lawrence, KS, pp. O430–O495.

Hessler, R. R. 1962. Secondary segmentation of the trilobite thorax. *J. Paleontol.* 36: 1305–1312.

Hintze, L. F. 1953. Lower Ordovician trilobites from western Utah and eastern Nevada. *Bull.-Utah Geol. Miner. Surv.* 48: 1–249.

Hu, C. H. 1971. Ontogeny and sexual dimorphism of Lower Paleozoic Trilobita. *Palaeontol. Am.* 44: 1–155.

Hughes, N. C. 2003a. Trilobite body patterning and the evolution of arthropod tagmosis. *BioEssays* 25: 386–395.

Hughes, N. C. 2003b. Trilobite tagmosis and body patterning from morphological and developmental perspectives. *Integr. Comp. Biol.* 41: 185–206.

Hughes, N. C., Chapman, R. E., and Adrain, J. M. 1999. The stability of thoracic segmentation in trilobites: a case study in developmental and ecological constraints. *Evol. Dev.* 1: 24–35.

Kobayashi, T. 1960. The Cambro-Ordovician formations and faunas of Sauth Korea, part VI, paleontology V. *J. Fac. Sci. Univ. Tokyo, Sec. 2* 12: 12: 217–275.

Kopaska-Merkel, D. C. 1987. Ontogeny and evolution of an Ordovician trilobite. *SEPM Mid-Year Meeting Abstr.* 4: 43–44.

Lee, D.-C., and Chatterton, B. D. E. 1997. Ontogenies of trilobites from the lower Ordovician Garden City Formation of Idaho and their implications for the phylogeny of the Cheirurina. *J. Paleontol.* 71: 683–702.

Ludvigsen, R. 1975. Ordovician formations and faunas, southern Mackenzie Mountains. *Can. J. Earth Sci.* 12: 663–97.

Ludvigsen, R., and Westrop, S. R. 1986. Classification of the Late Cambrian trilobite *Idiomesus* Raymond. *Can. J. Earth Sci.* 23: 300–307.

McNamara, K. J., Yu, F., and Zhou, Z. 2003. Ontogeny and heterochrony in the oryctocephalid trilobite *Arthricocephalus* from the Early Cambrian of China. *Spec. Pap. Palaeontol.* 70: 103–126.

Minelli, A., Fusco, G., and Hughes, N. C. 2003. Tagmata and segment specification in trilobites. *Spec. Pap. Palaeontol.* 70: 31–43.

Pratt, B. R. 1988. Continental margin reef tract of Early Ordovician age, Broken Skull Formation, Mackenzie Mountains, northwest Canada. In H. H. J. Geldsetzer, N. P. James, and G. E. Tebbutt (eds.). *Reefs: Canada and Adjacent Areas*, Vol. 13, Canadian Society of Petroleum Geologists, Calgary, Alberta, Canada, pp. 208–212.

Raymond, P. E. 1913. Notes on some new and old trilobites in the Victoria Memorial Museum, Canada Geological Survey (Ottawa). *Bull. Victoria Mem. Mus.* 1: 33–39.

Ross, R. J. Jr. 1951. Stratigraphy of the Garden City Formation in northeastern Utah, and its trilobite faunas. *Peabody Mus. Nat. Hist. Yale Univ.* 6: 1–161.

Ross, R. J. Jr., Hintze, L. H., Ethington, R. L., Miller, J. F., Taylor, M. E., and Repetski, J. E. 1997. The Ibexian, lowermost series in the North American Ordovician, with a section on echinoderm biostratigraphy, Sprinkle, J., and Guensberg T. E. In M. E. Taylor (ed.). *Early Paleozoic biochronology of the Great Basin, Western United States. US Geol. Surv. Prof. Pap.* 1579: 1–50.

Sadler, P. M., and Cooper, R. A. 2004. Calibration of the Ordovician timescale. In B. D. Webby, F. Paris, M. L. Droser, and I. G. Percival (eds.). *The Great Ordovician Biodiversification Event*. Columbia University Press, New York, pp. 48–51.

Salter, J. W. 1864. Figures and descriptions illustrative of British organic remains. *Mem. Geol. Surv. Great Britain* Decade 11. Trilobites (chiefly Silurian): 64.

Størmer, L. 1942. Studies on trilobite morphology, Part II. The larval development, the segmentation and the sutures, and their bearing on trilobite classification. *Norsk Geol. Tidsskr.* 21: 50–163.

Stubblefield, C. J. 1926. Notes on the development of a trilobite, *Shumardia pusilla* (Sars). *Zool. J. Linn. Soc. London* 35: 345–372.

Tipnis, R. S., Chatterton, B. D. E., and Ludvigsen, R. 1978. Ordovician conodont biostratigraphy of the southern District of Mackenzie, Canada. *Geol. Assoc. Can. Spec. Pap.* 18: 39–91.

Walch, J. E. I. 1771. *Die natuurlyke historie der versteeningen of uitvoerige afbeelding en beschryving van de versteende zaaken, die tot heden op den aardbodem zynontdekt*. J.C. Sepp, Amsterdam, pp. 11–145.

Waloszek, D., and Maas, A. 2005. The evolutionary history of crustacean segmentation: a fossil-based perspective. *Evol. Dev.* 7: 515–527.

Webster, M., Sheets, H. D., and Hughes, N. C. 2001. Allometric patterning in trilobite ontogeny: testing for allometric heterochrony in *Nephrolenellus*. In M. L. Zelditch (ed.). *Beyond Heterochrony*. Wiley-Liss, New York, pp. 105–144.

Whittington, H. B., and Evitt, W. R. 1953. Silicified Middle Ordovician trilobites. *Geol. Soc. Am. Mem.* 59: 1–137.